Synchronizing High-speed Optical Measurements with amateur equipment

Andre van Staden
andre@etiming.co.za

The purpose of this investigation is to demonstrate a low-cost method for measuring weak, rapid variable stellar flux with standard amateur class telescopes and CCD cameras. The nature of the flux under discussion is optical, periodic and in the millisecond time frame. Combining measurements spaced over a period of days to improve *signal to noise* (S/N) ratio is possible, but requires unprecedented timing accuracy, not common to optical astronomy (Eastman, J. et al. 2010). A typical related application is measuring signals from a pulsar in optical wavelengths. A low cost system will be introduced to demonstrate this technology, capable of resolving the light curve of the 16.5 magnitude pulsar in the Crab Nebula, with a 20cm telescope.

Introduction

High speed photometers (Straubmeier, C. et al., 2001; Nilsson, R. 2005) on large telescopes are the most common method for measuring high speed flux variability. Various Instruments and modes for using CCDs were also successfully applied for high-speed astrophysics in optical wavelengths. A list of such CCD techniques was compiled by Dhillon V.S. (2007). Unfortunately, this type instrumentation and technology is basically research related, associated with high cost and applied mostly by the professional domain. Another method is to use a stroboscopic system and a standard CCD and was thought to have potential for the amateur astronomer.

A stroboscopic system in terms of astronomical observations will periodically capture a timed fraction of the emission by means of a synchronizing shutter in front of the CCD. The shutter may be any controllable light interrupter but is usually a rotating wheel with cut-outs, synchronized to the frequency of the source. By controlling the frequency and phase of the shutter wheel, it is possible to resolve the phase or light curve by means of accurate CCD photometric measurements.

Stroboscopic systems were successfully applied to optical pulsar measurements in the past. A more recent paper by Cadez, A., et al, (2003) demonstrated resolving of the Crab pulsar light curve with a 2.12m telescope to a high degree with 9 degree cut-out widths on a chopper blade. The remainder of this paper will focus on a low cost, amateur version of the stroboscopic system with the necessary related tasks, capable of resolving the light curve of the Crab pulsar. The author believes that accurate timing is an essential ingredient associated with almost all high-speed photometry. This strobing system will provide an ideal opportunity to challenge and test the stringent timing accuracy.

The Crab Pulsar in the geocentric centre of the Crab Nebula (M1) rotates at approximately 30 revolutions per second and produces rapid fluctuations in intensity as the E-M beam sweeps across Earth. At a mean optical magnitude of 16.5, it was estimated to be a measurable target with a 20cm telescope and a ST9e CCD camera. Timing ephemeris for the Crab pulsar is published monthly and available from Jodrell Bank monthly ephemeris (Lyne, A.G.).

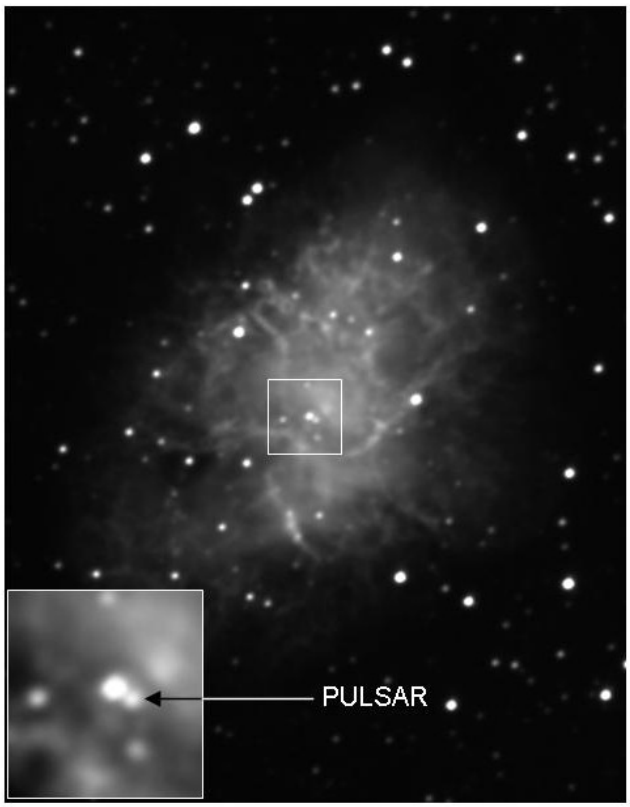

Fig. 1 Crab Nebula also known as M1. This image was captured by Axel Martin from Germany with a 30cm Newtonian Telescope and ST8XME CCD + CLS-Filter. The unprocessed image is the sum total of 3.5 hours of exposure time and shows the 16.5 Mag. pulsar (PSR 0534+2200) in the centre.

Concept

In principle, the frequency of the shutter has to be synchronized with the frequency of the pulsar at the telescope. Once the system is synchronized, it is possible to shift the phase of the shutter relative to the received signal and observe different fractions of the emission period. The size of the fractions or samples is determined by the open-to-close ratio of the shutter wheel. If for instance an open-to-close ratio of 1:2 is used, the measured flux will be an integral part of which the pulsar rotates an angle, 1/3 of its rotation period. The resolving resolutions of the pulsar light curve will be determined by the open-to-close ratio and the overall timing precision of the shutter phase over the accumulation period of many cycles.

In practice, the instantaneous phase of the shutter will always deviate from the assumed phase due to systematic errors. The shutter phase ϕ_S at time (t) can be written as:

$$\phi_S(t) = \phi_P(t) + T_{CORR}(t) + \delta T\phi_{CORR}(t) + \delta T_{sys} \quad (1)$$

Where $\phi_P(t)$ is the spin-down corrected phase of the pulsar at time (t) derived from ephemeris, $T_{CORR}(t)$ is the timing correction at time (t) to compensate for not observing from the Solar System Barycentre and other smaller timing issues, $\delta T\phi_{CORR}(t)$ are systematic errors involve to estimate $T\phi_{CORR}(t)$ and δT_{sys} are various system errors, e.g. mechanical tolerances. Constant errors resulting in a bias of $\phi_P(t)$ can be neglected for now but any variations or drifts from milliseconds to days must be dealt with and are discussed under **Shutter System** and **Timing Principals**, see below.

The design criteria were to keep ($\delta T\phi_{CORR}(t) + \delta T_{sys}$) < 1/100 of the Crab pulsar rotation period which relates to ~ 0.33 milliseconds timing error of $\phi_S(t)$. If this criterion can be met, it will be a possible to have a high number of narrow sampling windows spread over one period to resolve the light curve in great detail. For first trials a much lower sampling resolution was used with a shutter open-to-close ratio of only 1:2, but still tries to maintain the 0.33 milliseconds timing precision.

In theory the design incorporates a closed-loop system that does not accumulate timing errors (Fig. 2). The system starts with an estimated shutter frequency ($f_{EST} = 1/P_P(t)$) where $P_P(t)$ is the spin-down corrected period of the pulsar at time (t) derived from the ephemeris. The shutter optical interrupter produces a signal (S_i) on each rotation (i) of the disk that coincides with the mid-position of one of the four windows. The exact universal time, $Ts(i)$ for the signal is derived from a GPS Clock (Van Staden, A., 2013) smoothed by a $\alpha\beta$- smoothing algorithm and the corresponding phase $\phi_S(t)$ is calculated. This is compared to a pre-selected phase of interest, ϕ_{REF}. The difference ϕ_{REF-S} is the correction phase needed for f_{EST} to maintain

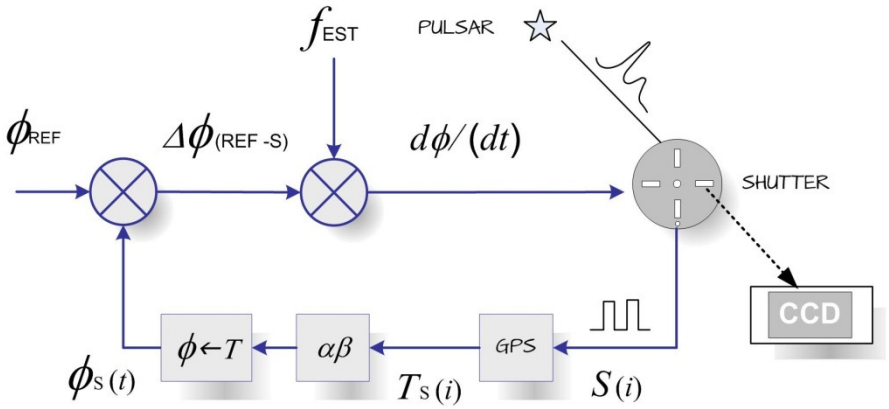

Fig. 2 Concept diagram

the shutter synchronization with the pulsar. To explore a new phase region simply means to dial-in a new reference phase, ϕ_{REF} and the closed-loop will automatic track on ϕ_{REF}.

Shutter System

The Shutter disk, 170mm diameter was made of a piece of Closed-Cell PVC foam board, also known as Forex (Wikipedia, 2013). A brushless DC (BLDC) motor from the hard drive of an old PC was stripped for the shutter motor. BLDC motors is a type of synchronous electric motor, small, lightweight, have high speed ranges are acoustically quiet and can be controlled almost like a stepper motor (Yedamale P., 2003).

Fig. 3 Shutter Housing and Shutter disk

The blade has four cut-outs equally spaced and translates to ~7.5 revolutions per second (~450 rpm) rotation speed when synchronized to the Crab pulsar frequency of 30 Hz (30 Hz/4 = 7.5 Hz). A pulse is produced once per revolution when sensor, **A** in the shutter housing coincident with a small hole **B** in the rotating disc.

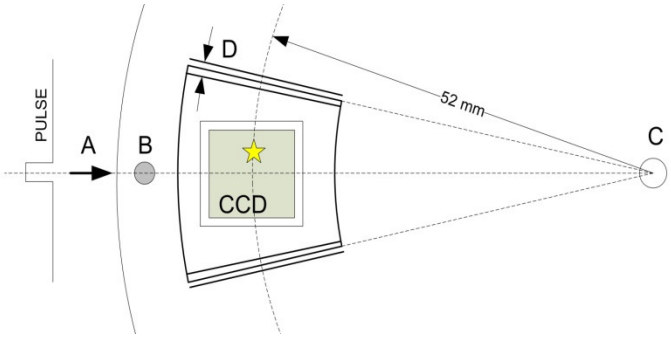

Fig. 4 Drawing of the Shutter disk with the CCD Chip in the background

In theory the centre of the pulse should reflect the instant when the geometric centre of the shutter window overlays the CCD and the image of the pulsar coincides with a line between AB and C (Fig. 4). Assuming the CCD centre coincides with the telescope optical axis then the amount of phase error $\delta T\phi_\psi$ resulting from the offset of the pulsar can be approximate by:

$$\delta T\phi_\psi \approx \left(\frac{4pF}{\pi r}\right) tan\left(\frac{\delta\psi}{2}\right) \quad (2)$$

where, p is the period of the pulsar, F is the effective focal length of the telescope, r is 52mm and $\delta\psi$ is angular offset of the pulsar from the CCD centre in the direction of rotation. Depending on the CCD orientation, mechanical tracking errors in the telescope drive system will modulate timing errors onto $\delta T\phi_\psi$. The same guide star at the same CCD position and orientation of the shutter-CCD assembly were maintained during the course of the measurement period to avoid phase errors.

Tolerances in the window dimensions (D) will also affect the expected and actual opening of the shutter. At a radius distance, r of 52mm from the centre of the disk and in the direction of rotation, the estimate timing error, δT_{dim} is:

$$\delta T_{dim} \approx \left(\frac{4p}{2\pi r}\right) = 0.42\ msec/mm \qquad (3)$$

where, p is the period of the pulsar. All measurements and cut-outs were made with tolerances kept in mind to agree with the design criteria of δT_{sys}.

Timing data $Ts(_i)$ (see *Fig 1*) were recorded and analyzed to measure random excitations of mechanical resonance in the motor-shutter system. The RMS error over a period of 30 minutes was 38.3 µsec. A frequency spectrum of the timing noise shows most of the power tends towards zero with a significant resonance peak at 1.78Hz.

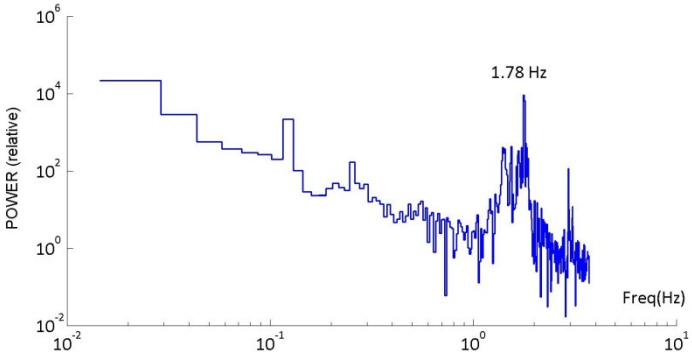

Fig. 5 FFT Frequency spectrum on logarithmic scales of the "mechanical" timing noise.

It was assumed that the excitations of the mechanical resonance originated from the hand-made disk and slight flexing of the disk. A laser-cut disk will probably be more suitable. The supply voltage on the BLDC motor also contributes to a constant phase offset and was calibrated before each observation session.

Timing Principles

Radio Observatories doing pulsar measurements are equipped with atomic time standards and modelling of accurate timing is a complex process. In support of this, the pulsar community has developed a state of the art (UNIX) program (over the past 40 years) called TEMPO II which models pulsar arrival times up to a accuracy of 1 ns. (Hobbs et al. 2006; Edwards et al.2006). For this accuracy, the exact positions of solar systems bodies must be known, only available through the online JPL Ephemeris system (Markwardt. C. ; JPL HORIZONS). However, for the proposed demonstration the computed (much less accurate) timing information in real-time with a program on a PC was used and only includes the most significant timing contributions.

The aim here is to determine the phase, $\phi(t)$ of the pulsar at a instance (t) related to the local UTC Clock. The phase of the pulsar can be determined from the monthly ephemeris but is only valid in the pulsar frame of reference (Lyne, A.G., et al.). An observer on Earth will measure a pulsar (close to the ecliptic) with a constant change in frequency due to the Doppler shift caused by the Earth's motion around the Sun and the spin of the Earth on its axis. Keeping book of timescales during observations is also important, for example the most common time standard, UTC is discontinuous and drifts with the addition of leap seconds (Eastman, J., et al., 2010). Also clocks on Earth are subject to relativistic effects and solar system gravitational influences will affect the timing.

The general approach here is to transform the measurements to the barycenter of the Solar System (Eastman, J., et al., 2010). The apparent time of an event has to be adjusted to be what it would be as if we were observing at the barycenter, which is the coordinate origin of all modern, precise astronomical positional calculations. If the source of the events is stationary with respect to the barycenter, this gives us a steady clock with which to measure when each event happened.

Transformation to the rest frame of the pulsar is achieved by transforming TOA (Time of Arrival) pulses to the barycentre and is the sum of various time corrections classically defined by

$$t_b = t + \Delta_C + \frac{\boldsymbol{r}\cdot\hat{\boldsymbol{n}}}{c} + \frac{(\boldsymbol{r}\cdot\hat{\boldsymbol{n}})^2 - |\boldsymbol{r}|^2}{2cd} - \frac{D}{f^2} + \Delta_{E\odot} + \Delta_{S\odot} + \Delta_{A\odot}, \qquad (4)$$

Where Δ_C contains various clock corrections, **r** is a vector from the barycentre to the telescope, $\hat{\boldsymbol{n}}$ is a unit vector pointing from the barycentre to the pulsar, c is the speed of light, d is the distance to the pulsar, D is the interstellar dispersion constant, f is the radio frequency, $\Delta_{E\odot}$ is the Einstein delay comprised of the gravitational red shift and time dilation, $\Delta_{S\odot}$ is the Shapiro delay characterising the curvature of space time near the Sun and $\Delta_{A\odot}$ is the aberration delay as a result of the Earth's rotation (Bell, J.F., 1996; Kaspi V.M; Lorimer D., 2008)

Terms three and four together make up the Roemer delay $\Delta_{R\odot}$. The 4th term can be ignored for now which applies only to nearby sources. The Roemer delay is the classical light travel time across the Earth's orbit, with a magnitude of ~500 $\cos\boldsymbol{\beta}$ seconds, where $\boldsymbol{\beta}$ is the ecliptic latitude of the pulsar (NRAO). With the Crab pulsar close to the ecliptic, the Doppler Effect is significant as the Earth passes through a couple of cycles during one evening (depending on the season). It is also interesting to note that a 0.1 arc second directional error can produce a timing error as high as 240 microseconds and it is therefore important to keep the pulsar's position in the same coordinate frame as the ephemeris. The geometric timing modulation due to the Earth's spin was compared between observations from the geocentric Earth and the (topocentric) observing site (Eastman, J., 2010).

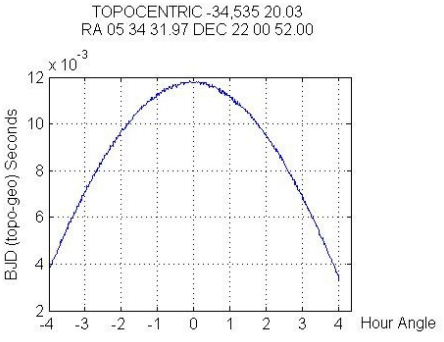

Fig. 6: Timing difference between topocentric and geocentric observing.

A portion around zero Hour Angle was plotted (Fig. 6) and reveals a substantial timing error if not corrected.

The dispersion delay, $\frac{D}{f^2}$ contributes at less than 1 μs in the optical band and can also be discarded (Eastman, J., et al., 2010). The $\Delta_{S\odot}$ and $\Delta_{A\odot}$ terms have magnitudes below the resolution of the design criteria and can be omitted as well. The Einstein delay can contain corrections as large as 1.6 milliseconds and have to be included.

Having made the above transformations, the observed phase is calculated. The frequency of the pulsar changes since the the pulsar loses energy through magnetic dipole radiation. By incorporating the spin-down parameters from ephemeris of one epoch, it is possible to calculate the phase $\phi(t)$ of the pulsar at a new time by the Taylor expansion

$$\phi(t) = \phi(0) + \nu(t - t_0) + \frac{1}{2}\dot{\nu}(t - t_0)^2 + \frac{1}{6}\ddot{\nu}(t - t_0)^3 + \ldots \quad (5)$$

where ν = 1/P is the rotational frequency, and $\dot{\nu}$, $\ddot{\nu}$ are the frequency derivatives corresponding to the spin-down parameters available from the ephemeris (Bell, J.F., 1996; Kaspi V.M; Lorimer D., 2008). Essentially, this formula calculates the integrated number of cycles over period ($t - t_0$) from a arbitrary reference t_0 and phase $\phi(0)$ where the phase is reflected in the fraction of the cycles.

Measuring Results

The concept was put to test on the Crab Pulsar during January and February 2013. Observations were made with the author's SBIG ST9e CCD camera and 20cm LX200 telescope.

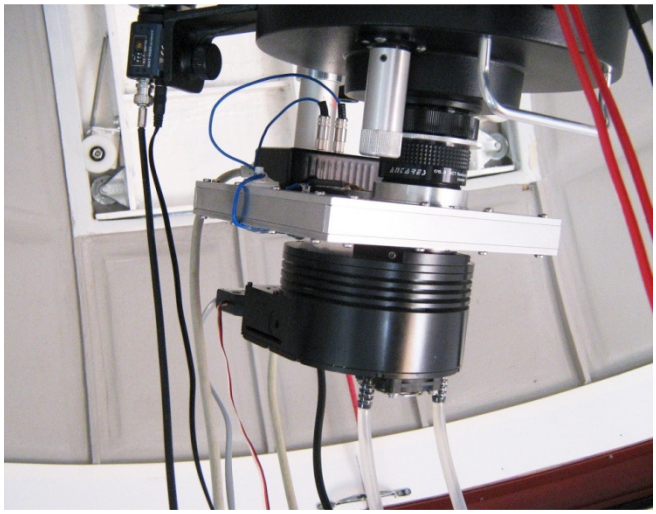

Fig. 7 The strobing assembly shown mounted between the 20cm SCT and ST9eCCD.

The cut-out shutter ratio of 1:2 produced a much lower resolution curve compared to the well established reference profile done with high speed photometers. The expected smoothed curve was calculated by convolving the window function with a reference profile of the Crab Pulsar, shown in Fig. 8. Photometric measurements at various phases of the pulsar period were performed and the resulted light curve was compared against the calculated profile.

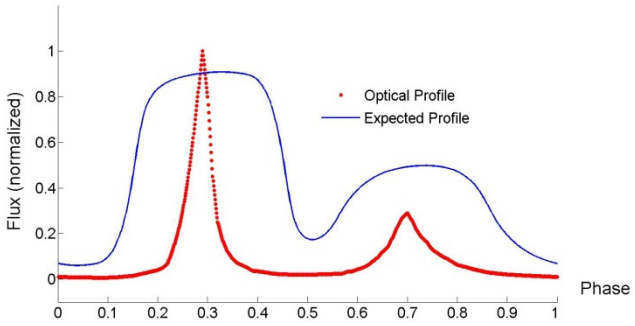

Fig. 8 The Optical Light curve of the Crab pulsar. The spatial integration function of the strobing Windows will result in measuring a smoothed light curve compare to measurements by high speed photometers. The expected smoothed curve is based on a 1:2 window opening.

Due to limited sky, and bad weather, only a maximum of about 5 measurement runs per evening was possible. A measurement run consists of 30 images with 30 second exposure each (total of 15 minutes) measuring a particular phase of the pulsar. The pulsar and the close companion star were not fully resolved in the 20-cm telescope: consequently photometry was performed on the combination with the pulsar periodically contribute to the photometric flux.

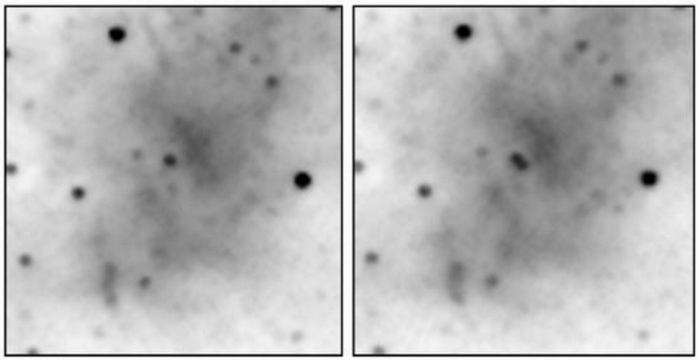

Fig. 9 CCD showing pulsar OFF and ON: 15 minute exposures with the stroboscope and the author's 20 cm / f10 telescope. Only 1/3 of the photons were collected making the effective exposure time actually 5 minutes. The left-hand panel shows the absence of the pulsar with about 9000 sample in its off-state. The pulsar, not fully resolved but visible in the right-hand panel resembles an accumulation of about 9000 pulses from the main lobe. Note that the pulsar is now almost the same magnitude as the close companion and disagree with other visual images of the pulsar. This is due to the fact that most of the pulsar's flux was captured while capturing only 1/3 of the "background".

All images were calibrated to standard protocol without the use of filters. It was found that images done above -15°C and effective exposures less than 900 seconds become unreliable for photometric measurements with the current system. Evening temperatures were around 24°C and the heat exchanging coolant had to be fed continuously with ice. Photometric measurements were performed with Astroart 5.0 (Nicolini,M., et al., 2013) and the USNO-B1 Catalog. This method had the disadvantage that the automatic centroid calculation by AstroArt 5.0 for the pulsar companion, slightly changed position during the "on"

and "off" state consequently overlays had different background areas on the nebula. A differential ensemble photometry was also performed where the centroid was only calculated once for the first image of the range of images (Henden, A., et al. 2009; Nicolini,M., et al., 2013; Romanishin, W., 2006). The instrumental magnitudes were then further processed and compared.

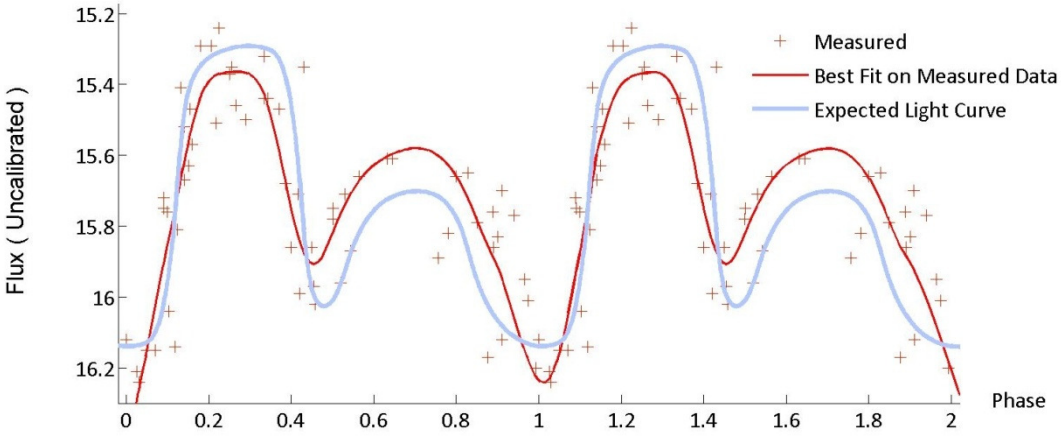

Fig. 10 The Crab Pulsar light curve compiled from 12 hours of photometric measurements during Jan/Feb 2013. The Cycle was repeated for illustration.

About 50 photometric measurements were performed during January and February 2013 and plotted (Fig. 10). A best fit through the data points was created and compared to the expected light curve. The expected light curve was scaled in the Y-Axis. The flux reading on the Y-Axis is not fully calibrated and is only an approximate magnitude. (At time of writing, there is still an unresolved issue where a correction for a 1 millisecond per day timing drift was manually applied in the light curve compilation.)

Conclusion

Initial attempts during 2011 and 2012 failed to converge in a light curve. This was mainly due to software issues and too low photometric S/N ratios. By further reducing the CCD temperature from -5°C to -15°C with a third stage cooling results in acceptable S/N ratios.

The BLDC motor and shutter disk performed above expectations considering its cost. A single desktop PC did all the timing calculation tasks, CCD captures and telescope control. The fast and accurate timing of the GPS clock played a key role in the system and effectively simplifies the concept.

The measured light curve (Fig. 10) shows an acceptable correlation and is therefore considered to be proof of the concept as presented. Although there is still room for timing improvements, it was shown that the timing was accurate enough to synchronize data over a two month period. It will be interesting if this period can be extending to have light curve continuity on following apparitions.

Additionally, the possibilities of detecting the pulsation of an object in particular star field were investigated. A Flux map was constructed for this purpose of 60 x 45 pixels, representing the normalized photometric measurements of 60 selected stars in 45 images of M1. The variability of the Crab pulsar shows up clearly as a vertical line in Fig. 11.

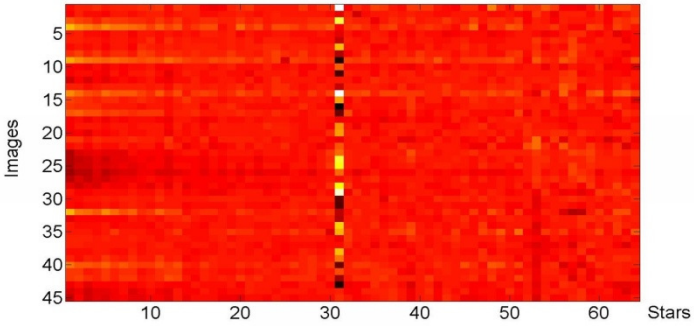

Fig. 11 Flux Map. By scaling Flux values it is easy to detect star fluctuations. The map consists of 45 images and 65 measured stars/image. The Crab pulsar is in star position 31.

Acknowledgments

I would like to thank Axel Martin (*Das Turtle Star Observatory, Germany*), for his long standing support, especially when it comes to photometric measurements. Thanks also to Ude Hertel, Hertel Precision Engineering, hertel@telkomsa.net, for his excellent job on the shutter housing and couplings.

References

Bell, JF, 1996. "Radio Pulsar Timing", *e-Print: arXiv:astro-ph/9610145v1*, 4-5.
Cadez, A, et al, 2003, "CCD based phase resolved stroboscopic photometry of pulsars", *e-Print: arXiv:astro-ph/0303368v1*, 1-4.
Dhillon, VS, et al, 2007, "ULTRACAM: an ultrafast, triple-beam CCD camera for high-speed Astrophysics", *MNRAS(2007)*, **378**, 2.
Eastman, J, et al, 2010, "Achieving Better Than 1 Minute Accuracy in the Heliocentric and Barycentric Julian Dates", *e-Print: arXiv:1005.4415v3*, 1, 2-7, 6, 7.
Henden, A, et al, 2009, "The AAVSO CCD Observing Manual", *e-Print: AAVSO(2009)*, 23.
Hobbs, GB, et al, 2006, **"**TEMPO 2, a new pulsar-timing package", *MNRAS (2006),* ***369,*** 1,
Kaspi VM, 1994, "High-Precision timing of millisecond pulsars and precision astrometry", *http://hdl.handle.net/2014/33528*, 3, 4.

Lorimer D, 2008, “Binary and Millisecond Pulsars*”, Living Rev. Relativity(2008) - ISSN 1433-8351*, **11**, 36, 37.
Lyne, AG, et al, 1993, “Jodrell Bank Crab Pulsar Timing Results, Monthly Ephemeris*”*, *MNRAS*, **265**, **1003**, http://www.jb.man.ac.uk/~pulsar/crab.html.
Straubmeier, C, et al, 2001, “OPTIMA: A Photon Counting High-Speed Photometer”, *Experimental Astronomy*, **11**, 4, 5.
Yedamale, P, 2003, “Brushless DC (BLDC) Motor Fundamentals”, *Microchip Technology Inc*, **AN885**, 1.

Related online sources:

Barycentric Julian Date, http://astroutils.astronomy.ohio-state.edu/time/bjd_explanation.html
Closed-cell PVC, http://en.wikipedia.org/wiki/Closed-cell_PVC_foamboard
How to read the JPL Ephemeris and Perform Barycentering, http://asd.gsfc.nasa.gov/Craig.Markwardt/bary/
Jodrell Bank Crab Pulsar Timing Results, Monthly Ephemeris, http://www.jb.man.ac.uk/~pulsar/crab.html
JPL HORIZONS - solar system data and ephemeris service, *http://ssd.jpl.nasa.gov/?horizons*
Nicolini,M, Astroart MSB Software, http://www.msb-astroart.com/
Nilsson, R, High-Speed Astrophysics: Chasing Neutron-Star Oscillations, http://www.scribd.com/doc/44046701/High-Speed-Astrophysics-Chasing-Neutron-Star-Oscillations
NRAO, Pulsar Timing Tutorial, www.cv.nrao.edu/course/astr534/PulsarTiming.html
Romanishin, W, 2006, An Introduction to Astronomical Photometry Using CCDs, http://www.physics.csbsju.edu/370/.../OU.edu_CCD_photometry_wrccd06.pdf
The AAVSO CCD Observing Manual, http://www.aavso.org/ccd-observing-manual
Van Staden, A, GPS E2 Clock, http://www.etiming.co.za